



## Full Length Article

# Characterization of biofuel refinery byproduct via selective electrospray ionization tandem mass spectrometry



Kelsey S. Boes<sup>a</sup>, Robert H. Narron<sup>b</sup>, Yufei Chen<sup>a</sup>, Sunkyu Park<sup>b</sup>, Nelson R. Vinuesa<sup>a,\*</sup>

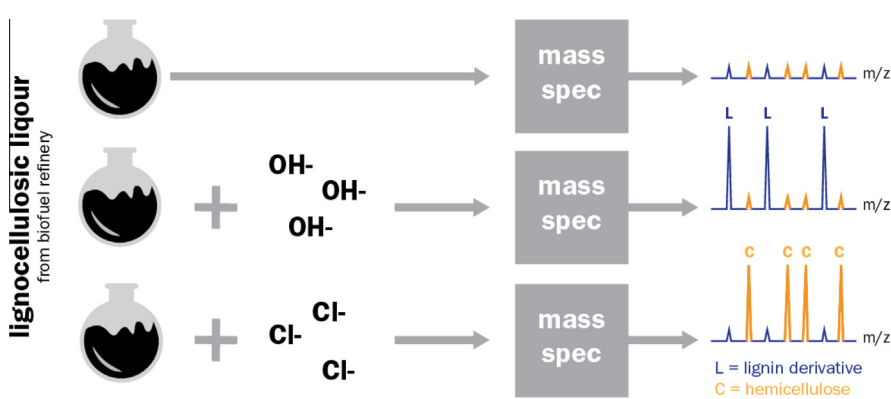
<sup>a</sup> Department of Textile Engineering, Chemistry, and Science, North Carolina State University, 1020 Main Campus Dr., Raleigh, NC 27606, United States

<sup>b</sup> Department of Forest Biomaterials, North Carolina State University, 2820 Faucette Blvd., Raleigh, NC 27607, United States

## HIGHLIGHTS

- Electrospray provides soft ionization of autohydrolyzate from 100 to 3200 m/z.
- Ionization dopants allow discrete analysis of cellulose and lignin sans separation.
- Chloride attachment in electrospray ionization assists in ionizing hemicellulose.
- Deprotonation by hydroxide specifically enhances ionization of lignin derivatives.

## GRAPHICAL ABSTRACT



## ARTICLE INFO

## Article history:

Received 6 July 2016

Received in revised form 16 September 2016

Accepted 2 October 2016

## Keywords:

Biomass pretreatment  
Tandem mass spectrometry  
Lignin  
Oligosaccharides  
Time-of-flight  
Electrospray ionization

## ABSTRACT

To achieve economic viability, biorefineries need to increase efficiency through characterization of byproducts for the purpose of valorization. One such byproduct is the liquid stream produced after autohydrolysis pretreatment, autohydrolyzate liquor, which contains valuable organic derivatives of hemicellulose and lignin from biomass. To characterize the autohydrolysis liquor, we employed a novel method for such liquor analysis that uses electrospray ionization and ion dopants in combination with tandem mass spectrometry using a quadrupole–time-of-flight mass spectrometer. Electrospray expands current analysis of such liquors through softer ionization. Ion dopants provide for differentiation of the complex mixture components without requiring derivatization or preliminary separation. The dopants—ammonium chloride and sodium hydroxide—primarily target and enhance ionization of hemicellulosic or lignin derivative species, respectively, based on the species' differing functionalities. Valuable structural information can be gleaned from these enhanced species by ion isolation and collision-activated dissociation (CAD), which reveals the presence of hemicellulosic or lignin derivative functionalities. These ionization techniques coupled with CAD enabled us to not only confirm the presence of low molecular weight ions, such as vanillin, as previously seen with gas chromatography–mass spectrometry but also expand the characterization to high molecular weight species. This expanded knowledge of the composition of autohydrolyzate liquor opens up the potential to develop lucrative co-products from this stream in a commercial biorefinery.

© 2016 Elsevier Ltd. All rights reserved.

*Abbreviations:* HPAEC, high-performance anion-exchange chromatography; HRMS, high resolution mass spectrometry; CAD, collision-activated dissociation; AH-L, autohydrolyzate liquor.

\* Corresponding author.

E-mail address: [nrvinuez@ncsu.edu](mailto:nrvinuez@ncsu.edu) (N.R. Vinuesa).

<http://dx.doi.org/10.1016/j.fuel.2016.10.016>

0016-2361/© 2016 Elsevier Ltd. All rights reserved.

## 1. Introduction

Biomass feedstocks are becoming a more investigated source of renewable energy as an alternative to fossil fuels [1]. Biorefineries have the possibility to produce sustainable and environmentally friendly sources of energy from lignocellulosic biomass feedstocks. Unfortunately, biorefineries are not yet efficient. In the case of ethanologenic biorefinery processes, only a fraction of the structural carbohydrates are actually converted into the final product. The rest of the conglomeration—unhydrolyzed cellulose microfibrils bundled with lignin and residual hemicellulosic polysaccharides [2]—is typically burned for heat or electricity production [3].

This lignin-rich mixture could be a step toward economic salience for the biofuel refineries. If the complex mixture could be separated, it would become a valuable product of the refinery [4]. Instead of being burned, the lignin should be valorized into co-product streams for raising the economic feasibility of a biorefinery process [5]. In addition to having a higher energy content than ethanol, lignin has many applications outside of biofuels from adhesives to cement additives [3]. It is also the largest source of renewable material with an aromatic phenolic backbone and could be used for the production of polymeric building blocks and valuable phenolic compounds [3]. Unfortunately, separation of lignin from the lignocellulosic biomass mixture is challenging and inhibited by a lack of knowledge of the exact make-up of the complex mixture. Future uses of lignin rely on good characterization of lignin and tailoring of separation treatments to yield valuable lignin products [6].

One of the leading pretreatment methods in terms of investigated techno-economic feasibility is autohydrolysis [7]. Utilizing only pressure and hot deionized water, autohydrolysis is known to disrupt the structures of the hemicellulose and lignin, enabling greater accessibility for depolymerizing cellulolytic enzyme systems. Notable benefits of utilizing autohydrolysis pretreatment in a biorefinery process include (1) the absence of reagent and associated recycling costs, (2) existing industrial-scale infrastructure capable of housing pretreatment (pulp mill pre-hydrolysis reactors), and finally (3) the potential value of the generated autohydrolyzate liquor, obtainable by solid-liquid separation.

Unfortunately, autohydrolyzate liquor (AH-L) is complex in nature and challenging to analyze fully with one instrument. Gas chromatography-mass spectrometry (GC-MS) analysis of ethyl acetate extract from dilute-acid hydrolyzate was shown to be an effective means of quantifying monomeric lignin fragments in hydrolyzate [8]. Despite this method's success, it is intrinsically limited by soluble-lignin's volatility within the applied column, hindering analysis of higher mass lignin fragments. Concerning hemicellulose-derived carbohydrates, GC-MS requires derivatization in the form of permethylation or acetylation to facilitate analysis [9]. Such derivatization, intended to simplify analysis, instead increases the variety of compounds present, making the mixture more complex and the spectrum more convoluted. The spectrum was made even more complex by the electron ionization (EI) coupled to the GC-MS. EI is a harsh ionization technique that typically fragments compounds, turning a single peak into several and rendering the molecular ions unobservable. A system utilizing high-performance anion-exchange chromatography (HPAEC) coupled with mass-spectrometry (MS) was capable of quantifying a variety of carbohydrates containing up to six residues in length [10]. However, the presence of unidentifiable peaks within the HPAEC-MS chromatograms again alludes to the less-than-complete characterization of pretreatment hydrolyzates that continues to occur in spite of great effort.

High resolution mass spectrometry (HRMS) and tandem mass spectrometry (MSMS) in concert with electrospray ionization

(ESI) and selective ionization dopants provide a means of successive characterization of both lignin- and hemicellulose-derived fragments soluble within AH-L. ESI, a soft ionization technique, enables ionization of higher mass compounds than ionizable with GC-EI-MS. GC-MS is limited by the volatility of the compounds and decomposition resulting from the temperature of the GC oven, which lowers its mass range; EI further encourages degradation of the compounds via fragmentation. The soft ionization of ESI overcomes the previously discussed challenges associated with complete characterization of AH-L.

Although HRMS is capable of differentiating thousands of components in an individual sample, there remain some hurdles to full analysis. One of the issues associated with such complex mixture analysis via mass spectrometry is ion suppression—a phenomenon where certain ions are less efficiently ionized and falsely appear at lower abundances in mass spectra or disappear altogether. It becomes necessary to tailor ionization in order to separately enhance the ionization efficiency of certain mixture components for several stages of analysis. Ammonium chloride (NH<sub>4</sub>Cl) and sodium hydroxide (NaOH) have been demonstrated to enhance ionization efficiency for hemicellulosic and lignin derivative species, respectively, in primarily model compound mixtures [11–13]. We combined these two techniques successively to analyze the wide variety of hemicellulosic species and then lignin derivative species present in AH-L, thereby minimizing the need for lengthy separation and extraction steps.

Once the targeted ions have been selectively enhanced, collision-activated dissociation (CAD) can be utilized to gain structural information. All ions except the target ions are filtered out by the quadrupole mass analyzer. Then the target ions are accelerated and collided with nitrogen gas to dissociate, or fragment, the ions. The resulting fragment ions—known as product ions—are recorded by the mass analyzer and reported in the CAD spectrum. With the higher resolving power afforded by the quadrupole time-of-flight (QTOF), we can determine the elemental composition of the fragments for structure elucidation.

In this study, ionization dopants were used to selectively enhance ionization of mixture components through gas phase basicity matching for simpler characterization of hardwood and non-wood AH-L. The resulting enhanced ionization—exhibiting up to a 30-fold increase in ion abundance for the targeted compounds—allowed for separate analysis of carbohydrates and lignin, respectively, without extraction or derivatization of the sample.

## 2. Experimental

### 2.1. Raw materials

All raw materials were air-dried at room temperature for two weeks to reach constant moisture. After air-drying, the moisture content of each biomass was determined by the mass loss after oven-drying overnight at 105 °C. Hardwood chips from red maple (*A. rubrum*) were obtained from the North Carolina State University Cooperative Tree Improvement Program and hand-cut to a size of 2 cm × 1 cm × 0.5 cm (length, width, thickness). The non-woody biomass, sugarcane bagasse, was kindly donated to the Department of Forest Biomaterials by a cooperating Brazilian bioenergy research institute. Before experimentation, both feedstocks were subjected to Soxhlet extraction utilizing an organic extraction solvent composed of 2:1 (v/v) benzene/ethanol. The purpose of this is to remove non-structural extractives that can hamper accurate analysis of results from the perspective of lignin. After 48 h of extraction, biomasses were air-dried under a fume hood and then stored in plastic bags at room temperature prior to pretreatment. In addition, part of the extractive-free feedstocks was ground by

a Wiley Mill (Model No. 4, Thomas Scientific, USA), and the sawdust was screened to particle size between 20 and 40 mesh. The screened raw sawdust was used for compositional analysis.

## 2.2. Autohydrolysis pretreatment

Autohydrolysis pretreatment was carried out in a 1.0 L alloy reactor (Parr Model C-276, Parr Instrument Company, USA). For each run, ~50 air-dry g of extractive-free biomass was loaded into the reactor and supplemented with the appropriate amount of deionized water (accounting for moisture content) to set the starting liquid to solids ratio to 10:1. To enhance mass and heat transfer, air in the reactor was removed via vacuum before heating. The target temperature was set at 180 °C and the average temperature ramp-up time was ~30 min. Target temperature was maintained for 40 min, followed by rapid temperature quenching in an ice water bath. After sufficient cooling, solid and liquid were separated by vacuum filtration using Whatman 40 grade filter paper. Residual liquid on the biomass was squeezed out by cheese cloth and filtered. Before analysis, autohydrolyzate liquor was centrifuged to separate the suspended solids which passed through the filter paper. The solids recovery yield was determined by measuring the total wet weight and the moisture content of pretreated samples, a necessary step for calculating changes to biomass composition before and after autohydrolysis pretreatment. Compositional analysis is performed in duplicate with all quantified components (carbohydrates, lignin, etc.) having relative percent differences of less than 0.5%.

## 2.3. Sample preparation for MS

The AH-L was filtered with Whatman 0.2 µm pore size filters and diluted 1:100 (AH-L/solvent) with water/methanol (50:50, v/v) to obtain a standard solution. Two mL of standard solution

were transferred to three different vials. No dopant was added to the first vial. To the second vial was added 0.2 mL of 25 mM NaOH to generate deprotonated molecules ( $[M-H]^-$ ). To the third was added 0.2 mL of 1 mM  $NH_4Cl$  to generate chloride-adducts (Cl-adduct,  $[M+Cl]^-$ ).

Lignin derivative standards were purchased from SigmaAldrich and used without further purification. Standards were dissolved to a concentration of 10 ppm with water/methanol (50:50, v/v). LC-MS grade methanol was purchased from J.T. Baker with a purity  $\geq 99.9\%$ .

## 2.4. Mass spectrometry

AH-L samples were analyzed using an Agilent Technologies 6520 Accurate-Mass QTOF LC/MS (Agilent, Santa Barbara, CA) equipped with an ESI source, operated in negative ion mode. The QTOF was operated in high resolution mode (4 GHz) with a resolving power ranging from 9700 for 100 m/z to 18,000 for 1600 m/z. The sample solution was injected into the ESI source using Harvard PhD 2000 Infusion syringe pump at a rate of 6 µL/min. The operating conditions for optimized ion formation consisted of nitrogen drying gas at a temperature of 355 °C and a rate of 12 L/min, 50 psig nebulizer, 90 V fragmentor voltage, 65 V skimmer voltage, 750 V octopole voltage, 3500 V Vcap voltage, and 0.029 µA capillary current. An injection time of one minute was used. To determine where the spectra transitioned from significant signal to noise, the injection time was increased to three minutes for an AH-L sample and a solvent blank of 50:50 water/methanol. The solvent blank was treated as a background and subtracted from the AH-L spectrum.

After being tentatively assigned, the Cl-adduct anions in the  $NH_4Cl$ -doped samples were subjected to CAD. Deprotonated molecules that demonstrated an increase in intensity in the NaOH-doped samples were subjected to CAD. Lignin derivative

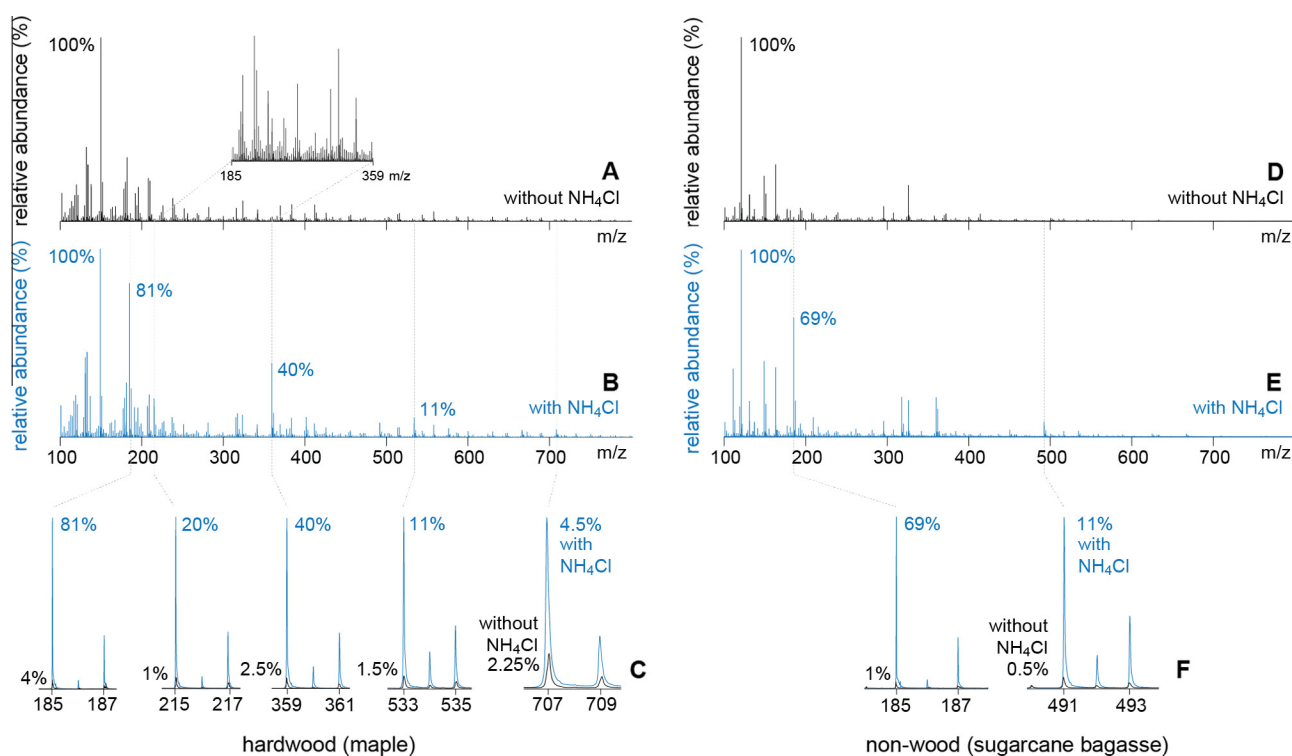


**Fig. 1.** Addition of  $NH_4Cl$  to AH-L generates Cl-adducts with carbohydrates that exhibit chlorine's characteristic 3:1 isotopic distribution in ESI-QTOF-MS spectra (B, E) as compared to the same sample with no  $NH_4Cl$  added (A, D), seen more explicitly upon magnification (C, F) with hardwood maple data displayed on the left (A, B, C) and non-wood sugarcane bagasse displayed on the right (D, E, F).

**Table 1**  
Cl-adduct ESI-MS and  $-MS^2$  hardwood maple AH-L ions of carbohydrates in AH-L.

| Assigned Formula<br>[mass error (ppm)]   | MS (m/z)   | $MS^2$ (m/z)  |
|--|--|---|
| $C_5H_{10}O_5 + Cl$ [1.5]  | $[M+Cl]^-$<br>(185.0214)   | 185–H <sub>2</sub> O (167)<br>185–H <sup>35</sup> Cl (149)<br>185–2(H <sub>2</sub> O) (149)   |
|  | $[M+Cl^{37}]^-$<br>(187.0950)  | 187–H <sub>2</sub> O (169)<br>187–H <sup>37</sup> Cl (149)  |
| $C_6H_{12}O_6 + Cl$ [0.5]  | $[M+Cl^{35}]^-$<br>(215.0321)  | 215–H <sub>2</sub> O (197)<br>215–H <sup>35</sup> Cl (179)  |
|  | $[M+Cl^{37}]^-$<br>(217.0457)  | 217–H <sup>37</sup> Cl (179)  |
| $C_{12}H_{20}O_{10} + Cl$ [0.8]  | $[M+Cl^{35}]^-$<br>(359.0742)  | 359–H <sub>2</sub> O (341)<br>359–H <sup>35</sup> Cl (323)<br>359–C <sub>6</sub> H <sub>10</sub> O <sub>5</sub> (197)   |
|  | $[M+Cl^{37}]^-$<br>(361.0732)  | 361–H <sub>2</sub> O (343)<br>361–H <sup>37</sup> Cl (323)  |
| $C_{19}H_{30}O_{15} + Cl$ [0.4]  | $[M+Cl^{35}]^-$<br>(533.1271)  | 533–C <sub>11</sub> H <sub>22</sub> O <sub>11</sub> (191)   |
|  | $[M+Cl^{37}]^-$<br>(535.1442)  | 535–C <sub>11</sub> H <sub>22</sub> O <sub>11</sub> (193)   |
| $C_{24}H_{38}O_{19} + Cl$ [4.8]  | $[M+Cl^{35}]^-$<br>(665.1728)  | 665–H <sup>35</sup> Cl (629)  |
|  |  | 665–H <sup>35</sup> Cl–C <sub>2</sub> H <sub>4</sub> O <sub>2</sub> –H <sub>2</sub> O (551)   |
|  |  | 665–H <sup>35</sup> Cl–C <sub>2</sub> H <sub>4</sub> O <sub>2</sub> –H <sub>2</sub> O–C <sub>3</sub> H <sub>4</sub> O <sub>2</sub> (479)  |
|  |  | 665–H <sup>35</sup> Cl–C <sub>2</sub> H <sub>4</sub> O <sub>2</sub> –H <sub>2</sub> O–C <sub>3</sub> H <sub>4</sub> O <sub>2</sub> –C <sub>2</sub> H <sub>2</sub> O (437)             |
|  |  | 665–H <sup>35</sup> Cl–2(C <sub>2</sub> H <sub>4</sub> O <sub>2</sub> )–H <sub>2</sub> O–C <sub>3</sub> H <sub>4</sub> O <sub>2</sub> –C <sub>2</sub> H <sub>2</sub> O (377)          |
|  |  | 665–H <sup>35</sup> Cl–2(C <sub>2</sub> H <sub>4</sub> O <sub>2</sub> )–H <sub>2</sub> O–2(C <sub>3</sub> H <sub>4</sub> O <sub>2</sub> )–C <sub>2</sub> H <sub>2</sub> O (305)       |
|  |  | 665–H <sup>35</sup> Cl–2(C <sub>2</sub> H <sub>4</sub> O <sub>2</sub> )–H <sub>2</sub> O–2(C <sub>3</sub> H <sub>4</sub> O <sub>2</sub> )–2(C <sub>2</sub> H <sub>2</sub> O) (263)    |
|  |  | 665–H <sup>35</sup> Cl–2(C <sub>2</sub> H <sub>4</sub> O <sub>2</sub> )–H <sub>2</sub> O–2(C <sub>3</sub> H <sub>4</sub> O <sub>2</sub> )–3(C <sub>2</sub> H <sub>2</sub> O) (221)    |
|  |  | 665–H <sup>35</sup> Cl–2(C <sub>2</sub> H <sub>4</sub> O <sub>2</sub> )–H <sub>2</sub> O–2(C <sub>3</sub> H <sub>4</sub> O <sub>2</sub> )–4(C <sub>2</sub> H <sub>2</sub> O) (179)    |
|  |  | 665–H <sup>35</sup> Cl–2(C <sub>2</sub> H <sub>4</sub> O <sub>2</sub> )–2(H <sub>2</sub> O)–2(C <sub>3</sub> H <sub>4</sub> O <sub>2</sub> )–4(C <sub>2</sub> H <sub>2</sub> O) (161) |
|  |  | 665–H <sup>35</sup> Cl–2(C <sub>2</sub> H <sub>4</sub> O <sub>2</sub> )–3(H <sub>2</sub> O)–2(C <sub>3</sub> H <sub>4</sub> O <sub>2</sub> )–4(C <sub>2</sub> H <sub>2</sub> O) (143) |
|  |  | 665–H <sup>35</sup> Cl–2(C <sub>2</sub> H <sub>4</sub> O <sub>2</sub> )–4(H <sub>2</sub> O)–2(C <sub>3</sub> H <sub>4</sub> O <sub>2</sub> )–3(C <sub>2</sub> H <sub>2</sub> O) (125) |
|  |  | 667–H <sup>37</sup> Cl–C <sub>2</sub> H <sub>4</sub> O <sub>2</sub> –H <sub>2</sub> O (551)   |
|  |  | 667–H <sup>37</sup> Cl–C <sub>2</sub> H <sub>4</sub> O <sub>2</sub> –H <sub>2</sub> O–C <sub>3</sub> H <sub>4</sub> O <sub>2</sub> (479)  |
|  |  | 667–H <sup>37</sup> Cl–C <sub>2</sub> H <sub>4</sub> O <sub>2</sub> –H <sub>2</sub> O–C <sub>3</sub> H <sub>4</sub> O <sub>2</sub> –C <sub>2</sub> H <sub>2</sub> O (437)             |
|  |  | 667–H <sup>37</sup> Cl–2(C <sub>2</sub> H <sub>4</sub> O <sub>2</sub> )–H <sub>2</sub> O–C <sub>3</sub> H <sub>4</sub> O <sub>2</sub> –C <sub>2</sub> H <sub>2</sub> O (377)          |
|  |  | 667–H <sup>37</sup> Cl–2(C <sub>2</sub> H <sub>4</sub> O <sub>2</sub> )–H <sub>2</sub> O–2(C <sub>3</sub> H <sub>4</sub> O <sub>2</sub> )–C <sub>2</sub> H <sub>2</sub> O (305)       |
| 667–H <sup>37</sup> Cl–2(C <sub>2</sub> H <sub>4</sub> O <sub>2</sub> )–H <sub>2</sub> O–2(C <sub>3</sub> H <sub>4</sub> O <sub>2</sub> )–2(C <sub>2</sub> H <sub>2</sub> O) (263) |  |   |
| $C_{26}H_{40}O_{20} + Cl$ [4.6]  | $[M+Cl^{35}]^-$<br>(707.1869)  | 707–H <sup>35</sup> Cl–C <sub>2</sub> H <sub>2</sub> O (629)  |
|  |  | 707–H <sup>35</sup> Cl–2(C <sub>2</sub> H <sub>2</sub> O) (587)   |
|  |  | 707–H <sup>35</sup> Cl–2(C <sub>2</sub> H <sub>2</sub> O)–2(H <sub>2</sub> O) (551)   |
|  |  | 707–H <sup>35</sup> Cl–2(C <sub>2</sub> H <sub>2</sub> O)–2(H <sub>2</sub> O)–C <sub>3</sub> H <sub>4</sub> O <sub>2</sub> (479)  |
|  |  | 709–H <sup>37</sup> Cl–2(C <sub>2</sub> H <sub>2</sub> O)–2(H <sub>2</sub> O) (551)   |
| $[M+Cl^{37}]^-$<br>(709.1978)  | 709–H <sup>37</sup> Cl–2(C <sub>2</sub> H <sub>2</sub> O)–2(H <sub>2</sub> O)–C <sub>3</sub> H <sub>4</sub> O <sub>2</sub> (479) |   |

Assigned chemical formulas [with mass errors (ppm)], Cl-adducts  $[M+Cl]^-$  observed (with m/z value), and the product ions of the Cl-adducts observed following high resolution  $MS^2$  (with m/z value).

standards were subjected to the same CAD as the AH-L. CAD experiments involved isolation of the anion by using a narrow ( $\sim 1.3$  m/z) window and acceleration of the anion to collide with nitrogen gas with collision energies 10–25 as defined by the MassHunter LC/MS Data Acquisition Workstation Software Version B.05.01 for 6200 series interface. Spectra were analyzed in profile mode with MassHunter Qualitative Analysis Workstation Software Version

B.06.00 interface. All CAD fragmentation presented in this manuscript is reported from analysis of hardwood maple AH-L. All experiments were run in triplicate.

### 3. Results and discussion

#### 3.1. Analysis of autohydrolysis liquors without dopant

Without an ionization dopant, the complex AH-L offers complicated mass spectra that are not easily analyzed. These could be painstakingly analyzed and characterized, but since the preponderance of analytes in solution obscures which signals are important and creates a convoluted spectrum, it would take significant research hours to identify each compound. Not to mention, it is possible that a specific molecule will not even be seen in the mass spectrum, making full characterization of AH-L impossible without method amendments [14]. This can partially be attributed to ion suppression, caused by mixture complexity, where a limited number of compounds can attain charge during ESI and therefore be detected by MS. It is also dictated by gas phase thermodynamics, which determine which ions are stable enough to reach the mass detector and therefore which compounds are seen in the spectrum and at what abundances [15]. The difference in gas phase basicity between the analyte anion and the dopant ion determines the stability of the analyte anion in negative-ion mode ESI-MS. A more stable charged anion will appear at higher abundance in the mass spectrum and be easier to identify; a less stable anion can disappear. To overcome these obstacles to analysis, we used ionization dopants to target certain compounds and increase their ion abundance above the rest for faster and simpler identification.

#### 3.2. Analysis of autohydrolysis liquors with ammonium chloride

In order to better analyze the carbohydrate oligomers in AH-L, an aqueous solution of  $NH_4Cl$  was added to the samples before ionization. With the addition of  $NH_4Cl$ , the intensity of certain signals in the mass spectrum increased, as can be seen in Fig. 1. Some of these signals exhibited the 3:1 isotopic ratio characteristic of a chloride anionic adduct, as observed in previous experiments [11,12]. This 3:1 ratio suggested that  $Cl^-$  from the dopant formed an adduct with a carbohydrate molecule in the AH-L. This can be rationalized by the similar gas phase basicity between a chloride anion and a deprotonated carbohydrate molecule as shown by Cai et al. [15]. The solution-phase affinity of the carbohydrate molecule for the  $Cl^-$  ion dictates the initial equilibrium between deprotonated molecule and Cl-adduct, but the stability of the Cl-adduct in the gas phase determines whether it will reach the detector. An anionic adduct will be more stable, the more similar the gas phase basicities of the adducting anion and deprotonated analyte. Deprotonated lignin does not have a similar gas phase basicity to  $Cl^-$  and therefore does not form a Cl-adduct. The spectra of the doped AH-L when compared to pure AH-L (Fig. 1) show a dramatic increase in intensity of the Cl-adducts. Ions of mass-to-charge (m/z) ratios 185.0214, 215.0321, 359.0742, 533.1271, and 707.1869 were identified as potential carbohydrate Cl-adducts in hardwood AH-L due to their 3:1 isotopic ratios. These ions saw increases in intensity by factors of  $18.5 \pm 1.4$ ,  $15.2 \pm 0.4$ ,  $15.8 \pm 1.1$ ,  $12 \pm 2$ , and  $4.8 \pm 0.2$ , respectively, upon addition of  $NH_4Cl$ . The latter four ions were only present at relative abundances below 1.4% during analysis without dopant.

To ensure the observed 3:1 isotopic ratios were derived from Cl-attachment, CAD was performed on the selected ions in hardwood maple AH-L. Cl-adducts typically lose hydrogen chloride (HCl) when subjected to CAD [12]. We, therefore, monitored for the loss of  $H^{35}Cl$  and  $H^{37}Cl$  when targeting the M and M+2 peaks

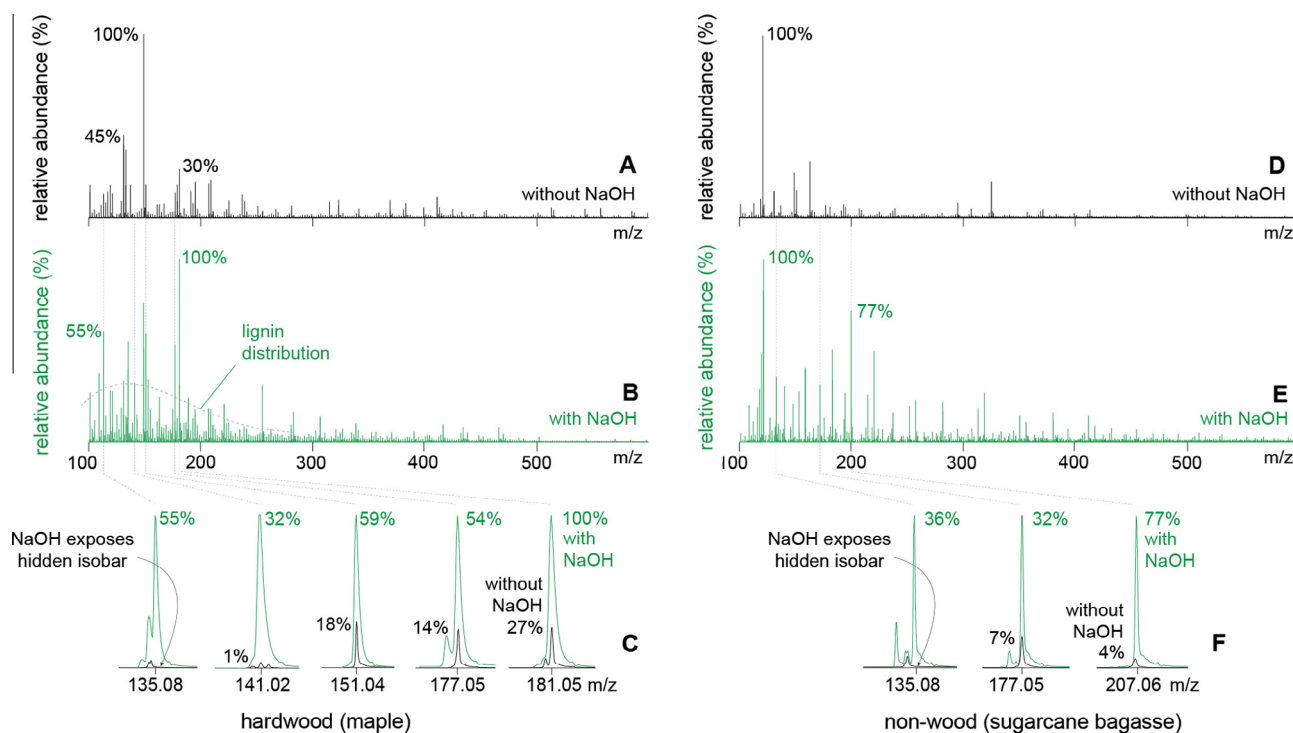


**Fig. 2.** Addition of sodium hydroxide (NaOH) to AH-L increases the intensity of lignin derivative ions in ESI-QTOF-MS spectra (B, E) as compared to the same sample with no NaOH added (A, D), seen more explicitly upon magnification (C, F) with hardwood maple data displayed on the left (A, B, C) and non-wood sugarcane bagasse displayed on the right (D, E, F).

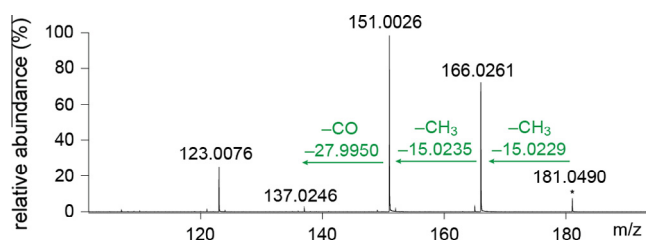


**Fig. 3.** Fragmentation of hardwood maple AH-L peak exhibiting enhanced ion abundance upon addition of NaOH (Table 2) matches that of characteristic lignin derivative fragmentation as seen in Table 3.

respectively, confirming by exact mass measurements that the ions were Cl-adducts and therefore carbohydrates. The Cl-adducts also demonstrated fragmentation characteristic of carbohydrates observed previously [12]. By preliminary CAD, we see that the sugarcane bagasse AH-L behaves similarly to the hardwood maple AH-L by forming Cl-adducts with carbohydrates for comparable enhancement of signals.

With the precision of the Q-TOF,  $m/z$  ratios can be determined with a mass error below 5 ppm. This accuracy allows assignment of chemical formulas associated with a signal by summation of exact masses of the possible elements in the molecule. Table 1 contains the calculated chemical formulas for the Cl-adduct peaks in hardwood AH-L and the ppm error, using the following suggested constraints of elements and numbers of each element for deprotonated and chlorinated anions below 1000  $m/z$ : C (0–78), H (0–126), O (0–20), Cl (0–12), N (0–20) [16]. Equal to or less than 5 ppm error is considered acceptable based on manufacturer specifications and instrument performance. The weightier two carbohydrate ions—533.1271 and 707.1869—are most likely products of ring cleavage of a larger carbohydrate oligomer, as is common [12]. Although neither the 533 nor the 535 ion display HCl loss,

we conclude that they contain Cl-adducts because both ions exhibit cellobiose loss while retaining their  $m/z$  difference of two, which implies that the Cl-adducts remain intact during CAD as has been previously observed in sucrose [12]. The ion with highest abundance in both spectra in Fig. 1—149.0446  $m/z$ —is attributed to deprotonated xylose, as confirmed by CAD of the xylose Cl-adduct ion at 185.0214  $m/z$ .

**Table 2**

Deprotonated ESI/MS and  $MS^2$  ions in hardwood maple AH-L that increased with intensity upon addition of NaOH.

| Assigned formula (M)<br>[mass error (ppm)] | MS ( $m/z$ )         | $MS^2$ ( $m/z$ )   |
|--|----------------------|--|
| $C_9H_{12}O$ [−1.8]                        | $[M-H]^-$ (135.0818) | 135-CO (107)<br>135- $CH_3$ (120)  |
| $C_6H_6O_4$ [−0.1]                         | $[M-H]^-$ (141.0188) | 141- $CH_3$ (125)<br>141-2( $CH_3$ ) (111)<br>141- $H_2O$ (122)                    |
| $C_8H_8O_3$ [0.5]                          | $[M-H]^-$ (151.0396) | 151- $CH_3$ (136)<br>151- $CH_3$ -CO (108)   |
| $C_{10}H_{10}O_3$ [4.3]                    | $[M-H]^-$ (177.0544) | 177- $CH_3$ (162)<br>177- $CH_3$ -CO (134)   |
| $C_9H_{10}O_4$ [3.8]                       | $[M-H]^-$ (181.0499) | 181- $CH_3$ (166)<br>181-2( $CH_3$ ) (151)<br>181-2( $CH_3$ )-CO (123)             |
| $C_{11}H_{14}O_5$ [−1.3]                   | $[M-H]^-$ (225.0766) | 225- $CH_3$ (210)<br>225- $CH_3$ - $CH_2O$ (180)<br>225-2( $CH_3$ )- $CH_2O$ (165) |
| $C_{22}H_{26}O_8$ [4.2]                    | $[M-H]^-$ (417.1532) | 417- $CH_3$ (402)<br>417-2( $CH_3$ ) (387)   |

Deprotonated anions  $[M-H]^-$  observed (with  $m/z$  value) and the product ions of the anions observed following high resolution  $MS^2$  (with  $m/z$  value).

### 3.3. Analysis of autohydrolysis liquors with sodium hydroxide

To enhance analysis of lignin derivatives in the AH-L, an aqueous solution of NaOH was added. Hydroxide enhances ion abundance of lignin derivatives over carbohydrates by inducing deprotonation. An ionization bias occurs toward phenolics because the more acidic phenolic hydrogen ( $pK_a \sim 6\text{--}10$ ) is thermodynamically favored to be deprotonated compared to the hydrogen on the carbohydrate alcohol ( $pK_a 16\text{--}18$ ) [17]. Up to a 30-fold increase in intensity of lignin derivative ions was observed in both hardwood (Fig. 2B) and non-wood AH-L (Fig. 2D). The utility of hydroxide as a dopant is especially exhibited in the peak at 135.08 m/z, seen in Fig. 2C and F, where the lignin derivative peak of interest was unresolved and hidden within an isobaric ion. Addition of hydroxide brought the peak into view, increasing the relative abundance to 55% and 36% for hardwood and non-wood, respectively. The mélange of peaks also converged into a more readily identifiable distribution in hardwood maple AH-L. Compounds like lignin display distributions such as these, rather than individual peaks, because they are comprised of a conglomeration of molecules ranging in mass from one tail of the distribution to the other. Because the molecules below 100 m/z are already easily analyzed by GC-MS, we have tuned our mass spectrometer to scan from 100 to 3200 m/z. This means the low mass end of the distribution below 100 m/z is not visible to us. The high mass end of the distribution trails off at  $\sim 600$  m/z. After subtracting a solvent blank from the spectrum, we observed signals with a signal-to-noise ratio greater than 3:1 continuing up to 1275 m/z. However, these enhanced signals above 600 m/z can be primarily attributed to ion clusters, as confirmed by CAD (see Fig. 1SM).

To confirm that the signals with increased intensities were lignin derivatives, the signals in hardwood maple AH-L were subjected to CAD (Fig. 3) and their fragmentation was compared to that of lignin derivative standards. The enhanced signals exhibited fragmentation characteristic of lignin derivatives based on our experiments and previous studies of lignin and carbohydrate fragmentation [18]. For example, one of the signals that increased in intensity in hardwood AH-L (181.0499 m/z) was confirmed to be

deprotonated syringaldehyde (181.0501 amu). Upon CAD, the ion at 181.0499 m/z exhibited two methyl losses followed by loss of a carbonyl group as seen in Fig. 3. This is identical to the fragmentation exhibited by syringaldehyde (Table 3). Another signal (151.0396 m/z) was confirmed to be deprotonated vanillin (151.0395 amu) with both exhibiting methyl loss followed by CO loss. Every fragmented AH-L peak that increased upon addition of hydroxide exhibited loss of a methyl group, which is not seen in carbohydrate fragmentation [18]. The majority also exhibited CO loss, which was a common fragment found in our fragmentation of lignin derivative standards and in previous studies [18]. The full results of hardwood AH-L CAD experiments can be found in Table 2 and compared to CAD of lignin derivative standards in Table 3. Preliminary CAD indicates that non-wood sugarcane bagasse behaves similarly to hardwood maple AH-L with lignin derivatives being enhanced upon addition of hydroxide. The enhanced signal at 207.0668 m/z (assigned formula  $C_{11}H_{12}O_4$ , 2.5 ppm) in non-wood AH-L exhibited loss of methyl and loss of CO, consistent with lignin derivative fragmentation.

### 3.4. Current extent of autohydrolysis pretreatment characterization

The insufficiencies of conventional compositional analysis of biomass pose challenges to fully-describing the quantity of structural biopolymers (carbohydrates and lignin derivatives) which compose a given raw biomass feedstock [19]. However, complete characterization of biomass feedstocks is important. Establishing a replicable mass balance from both solid and liquid fractions generated after autohydrolysis of raw biomass is vital for full understanding of the effect of autohydrolysis upon raw lignocellulosic biomass. Furthermore, exact quantitation of a feedstock's raw composition is indispensable toward calculating the recovery of different solid and liquid components after autohydrolysis. As can be seen in Table 4, the total mass of each quantified component for raw biomass—87.6% and 93.4%—is less than that of AH-solid—95.2% and 96.0%—for maple and sugarcane bagasse, respectively. These numbers can be improved through extended characterization of AH-L. Table 4 presents the current extent of

**Table 3**  
Deprotonated ESI/MS and MS<sup>2</sup> ions in lignin derivative standards.

| Analyte (M) [mass error (ppm)]  | Exact mass (amu) | MS (m/z)                      | MS <sup>2</sup> (m/z)  |
|---|------------------|-------------------------------|--|
| 2-Hydroxybenzyl alcohol (C <sub>7</sub> H <sub>8</sub> O <sub>2</sub> ) [−3.6]            | 124.0524         | [M−H] <sup>−</sup> (123.0452) | 123−H <sub>2</sub> O (105)   |
| Guaiacol (C <sub>7</sub> H <sub>8</sub> O <sub>2</sub> ) [4.9]                            | 124.0524         | [M−H] <sup>−</sup> (123.0446) | 123−CH <sub>3</sub> (108)<br>123−H <sub>2</sub> O (105)  |
| 2-Methoxy-4-methylphenol (C <sub>8</sub> H <sub>10</sub> O <sub>2</sub> ) [1.8]           | 138.0681         | [M−H] <sup>−</sup> (137.0605) | 137−CH <sub>3</sub> (122)<br>137−CO (109)<br>137−HOCH <sub>3</sub> (105)   |
| Vanillin (C <sub>8</sub> H <sub>8</sub> O <sub>3</sub> ) [1.5]                            | 152.0473         | [M−H] <sup>−</sup> (151.0399) | 151−CH <sub>3</sub> (136)<br>151−CH <sub>3</sub> −CO (108)   |
| Vanillic acid (C <sub>8</sub> H <sub>8</sub> O <sub>4</sub> ) [−0.1]                      | 168.0423         | [M−H] <sup>−</sup> (167.0351) | 167−CH <sub>3</sub> (152)<br>167−CH <sub>3</sub> −CO <sub>2</sub> (108)<br>167−CO <sub>2</sub> (123)   |
| Eugenol (C <sub>10</sub> H <sub>11</sub> O <sub>2</sub> ) [3.6]                           | 164.0837         | [M−H] <sup>−</sup> (163.0765) | 163−CH <sub>3</sub> (148)  |
| Syringaldehyde (C <sub>9</sub> H <sub>10</sub> O <sub>4</sub> ) [−4.1]                    | 182.0579         | [M−H] <sup>−</sup> (181.0514) | 151−CH <sub>3</sub> (166)<br>151−2(CH <sub>3</sub> ) (151)<br>151−2(CH <sub>3</sub> )−CO (123)<br>151−CH <sub>3</sub> −CHO (137)   |
| Guaiacylglycerol-β-guaiacyl ether (C <sub>17</sub> H <sub>19</sub> O <sub>6</sub> ) [4.6] | 320.1260         | [M−H] <sup>−</sup> (319.1172) | 319−H <sub>2</sub> O−CH <sub>2</sub> O (271)<br>319−H <sub>2</sub> O−CH <sub>2</sub> O−CH <sub>3</sub> (256)<br>319−H <sub>2</sub> O−CH <sub>2</sub> O−C <sub>6</sub> H <sub>5</sub> OCH <sub>3</sub> −CH <sub>3</sub> (149)<br>319−2(H <sub>2</sub> O)−3(CH <sub>2</sub> O)−CH <sub>3</sub> (150)<br>319−2(H <sub>2</sub> O)−3(CH <sub>2</sub> O)−CH <sub>3</sub> −CO (122) |

Exact mass of standard, deprotonated anion [M−H]<sup>−</sup> of standard observed (with m/z value), and the product ions of the standard observed following high resolution MS<sup>2</sup> (with m/z value).

**Table 4**  
Mass balances from autohydrolysis pretreatment.

| Biomass                     | Weight<br>(g/100 g extractive-free raw biomass) | Glucan (g)                           | Xylan (g)                             | Minor Sugars (g)                     | Lignin (g)                          | Ash (g) | Total<br>(g/100 g solid sample) |
|-----------------------------|---|--------------------------------------|---------------------------------------|--------------------------------------|-------------------------------------|---------|---------------------------------|
| Maple, raw                  | 100   | 44.1                                 | 13.3                                  | 4.2                                  | 25.7                                | 0.3     | 87.6%                           |
| Maple, AH-Solid             | 69.2  | 40.1                                 | 3.0                                   | 1.5                                  | 21.3                                | 0.0     | 95.2%                           |
| Maple, AH-L                 | 30.8 (+1000 g H <sub>2</sub> O)                 | M 0.6<br>T 1.1<br>O <sup>a</sup> 0.5 | M 2.9<br>T 9.4<br>O <sup>a</sup> 6.5  | M 1.4<br>T 2.5<br>O <sup>a</sup> 1.1 | 3.9, <sup>b</sup> 0.03 <sup>c</sup> | –       | –                               |
| Sugarcane bagasse, raw      | 100   | 44.0                                 | 21.7                                  | 3.6                                  | 21.3                                | 2.8     | 93.4%                           |
| Sugarcane bagasse, AH-Solid | 59.0  | 37.3                                 | 3.5                                   | 0.4                                  | 14.0                                | 1.4     | 96.0%                           |
| Sugarcane bagasse, AH-L     | 41.0 (+1000 g H <sub>2</sub> O)                 | M 0.4<br>T 1.9<br>O <sup>a</sup> 1.5 | M 1.4<br>T 10.4<br>O <sup>a</sup> 9.0 | M 1.6<br>T 2.8<br>O <sup>a</sup> 1.2 | 6.5, <sup>b</sup> 0.16 <sup>c</sup> | –       | –                               |

<sup>a</sup> Monomeric, Total, and Oligomeric (by difference) Sugar Concentrations after AH-L Oligosaccharide Acid Hydrolysis (4% H<sub>2</sub>SO<sub>4</sub>, 1 h, 121 °C).

<sup>b</sup> Soluble Lignin Concentration by Difference in Weight and Composition of Solid Biomass.

<sup>c</sup> Lignin monomer concentrations determined according to method published by Mitchell.<sup>[8]</sup>

characterization for the hardwood and non-wood biomasses used in this study [20]. By using the dopants explored in this study, we hope to extend and improve the characterization of AH-L, which will expand our understanding of the effect of autohydrolysis on raw biomass.

#### 4. Conclusion

AH-L from hardwood maple and non-wood sugarcane bagasse were analyzed via high resolution MS. Dopants assisted in the selective optimization of ionization of different components and allowed for separate analysis of various portions of the mixture without extraction or extensive sample preparation. NH<sub>4</sub>Cl was used to identify carbohydrates through chloride adduction. The 3:1 isotopic ratio of chlorine made it simple to detect and target the carbohydrate peaks with CAD in order to confirm Cl-attachment and facilitate further structure elucidation. Sodium hydroxide enhanced the ionization of lignin species, increasing the ion abundance of lignin compounds up to 30-fold and resolving a distribution. Ions which increased in intensity upon addition of NaOH were confirmed in hardwood maple AH-L to be lignin derivatives by comparison of CAD results with those of lignin derivative standards. Ongoing work is being carried out to determine the effect of these dopants on AH-L from various biomasses. The detailed information obtainable through tailored ionization and CAD will enable greater understanding of the effect of autohydrolysis on biomass and future modification of the autohydrolysis process for extraction of desired compounds.

#### Notes

The authors declare no competing financial interest.

#### Acknowledgments

This interdepartmental project is generously supported by the North Carolina State Startup Fund, the North Carolina

Biotechnology Center (Grant No. 2016-BIG-6514), and the USDA National Institute of Food and Agriculture (Grant No. 2011-68005-30410).

#### Appendix A. Supplementary material

Supplementary data associated with this article can be found, in the online version, at <http://dx.doi.org/10.1016/j.fuel.2016.10.016>.

#### References

- [1] Galembeck F. *Energy Environ Sci* 2010;3(4):393.
- [2] Cesarino I, Araújo P, Domingues Júnior AP, Mazzafera P. *Braz J Bot* 2012;35(4):303–11.
- [3] Ten E, Vermerris W. *J Appl Polym Sci* 2015;132(24):1–13.
- [4] Yuan TQ, Xu F, Sun RC. *J Chem Technol Biotechnol* 2013;88(3):346–52.
- [5] Narron RH, Kim H, Chang H, Jameel H, Park S. *Curr Opin Biotechnol* 2016;38:39–46.
- [6] Fachuang L, Ralph J. *J. Biobased Mater Bioenergy* 2011;5:169–80.
- [7] Han Q, Jin Y, Jameel H, Chang H-M, Phillips R, Park S. *Appl Biochem Biotechnol* 2015;175(2):1193–210.
- [8] Mitchell VD, Taylor CM, Bauer S. *Bioenergy Res* 2014;7(2):654–69.
- [9] Björndal H, Lindberg B, Svensson S. *Carbohydr Res* 1967;5:433–40.
- [10] Coulier L, Zha Y, Bas R, Punt PJ. *Bioresour Technol* 2013;133:221–31.
- [11] Vinueza NR, Gallardo VA, Klimek JF, Carpita NC, Kenttämäa HI. *Carbohydr Polym* 2013;98(1):1203–13.
- [12] Vinueza NR, Gallardo VA, Klimek JF, Carpita NC, Kenttämäa HI. *Fuel* 2013;105:235–46.
- [13] Hauptert LJ, Owen BC, Marcum CL, Jarrell TM, Pulliam CJ, Amundson LM, Narra P, Aqueel MS, Parsell TH, Abu-Omar MM, Kenttämäa HI. *Fuel* 2012;95:634–41.
- [14] Kebarle P, Tang L. *Anal Chem* 1993;65(22):972A–86A.
- [15] Cai Y, Cole RB. *Anal Chem* 2002;74(5):985–91.
- [16] Kind T, Fiehn O. *BMC Bioinformatics* 2007;8:105.
- [17] Ragnar M, Lindgren CT, Nilvebrant NOJ. *Wood Chem Technol* 2000;20(3):227–305.
- [18] Morreel K, Kim H, Lu F, Dima O, Akiyama T, Vanholme R, Niculacs C, Goeminne G, Inzé D, Messens E, Ralph J, Boerjan W. *Anal Chem* 2010;82(19):8095–105.
- [19] Sluiter J, Sluiter A. *Summative Mass Closure: Laboratory Analytical Procedure (LAP) Review and Integration: Feedstocks*; Issue Date: April 2010; Revision Date: July 2011 (Version 07-08-2011); 2010.
- [20] Han Q, Jin Y, Jameel H, Chang H min, Phillips R, Park S. *Appl Biochem Biotechnol* 2014;175(2):1193–210.